ADVANCES IN ATMOSPHERIC SCIENCES, VOL. 34, JUNE 2017, 713–726

• **Original Paper** •

A Trend towards a Stable Warm and Windless State of the Surface Weather Conditions in Northern and Northeastern China during 1961–2014

Bo SUN*[1,2,3] and Huijun WANG[1,3]

[1]*Collaborative Innovation Center on Forecast and Evaluation of Meteorological Disasters, Nanjing University of Information Science and Technology, Nanjing* 210044*, China*

[2]*International Pacific Research Center and Department of Atmospheric Sciences, University of Hawaii at Manoa, Honolulu, HI* 96822*, USA*

[3]*Nansen-Zhu International Research Centre, Institute of Atmospheric Physics, Chinese Academy of Sciences, Beijing* 100029*, China*

(Received 5 October 2016; revised 26 February 2017; accepted 27 February 2017)

ABSTRACT

This study investigates the trends in the mean state and the day-to-day variability (DDV) of the surface weather conditions over northern and northeastern China (NNEC) during 1961–2014 using CN05.1 observational data. In this study, we show that the surface temperature (wind speed) has increased (decreased) over NNEC and that the DDV of the surface temperatures and wind speeds has decreased, indicating a trend towards a stable warm and windless state of the surface weather conditions over NNEC. This finding implies a trend towards more persistent hot and windless episodes, which threaten human health and aggravate environmental problems. The trends are also examined in reanalysis data. Both the ERA-40 and the NCEP data show an increasing (decreasing) trend in the mean state of the surface temperatures (wind speeds). However, the reanalysis data show a consistent decreasing trend in the DDV of the surface weather conditions only in the spring. The underlying reason for the decreased DDV of the surface weather conditions is further analyzed, focusing on the spring season. Essentially, the decreased DDV of the surface weather conditions can be attributed to a decrease in synoptic-scale wave activity, which is caused by a decrease in the baroclinic instability. There is a contrasting change in the baroclinic instability over East Asia, showing a decreasing (increasing) trend north (south) of 40°N. This contrasting change in the baroclinic instability is primarily caused by a tropospheric cooling zone over East Asia at approximately 40°N, which influences the meridional temperature gradient over East Asia.

Key words: day-to-day variability, surface weather condition, trend, northern and northeastern China

Citation: Sun. B., and H. J. Wang, 2017: A trend towards a stable warm and windless state of the surface weather conditions in northern and northeastern China during 1961–2014. *Adv. Atmos. Sci.*, **34**(6), 713–726, doi: 10.1007/s00376-017-6252-x.

1. Introduction

During the past several decades, a warming trend and a declining wind speed trend have been observed over China (Lin et al., 2013; Ji et al., 2014; Zhao et al., 2014; Wu et al., 2017). The warming over China has mainly been attributed to increasing greenhouse gas emissions (Ding et al., 2007). Specifically, Zhao et al. (2014) argued that the warming over East China is closely related to the sea surface temperature of the tropical Indian Ocean and atmospheric circulations over Siberia. The declining wind speed may also be a result of global warming, which causes weakened atmospheric circulation by weakening the temperature and pressure gradients between the East Asian continent and the adjacent oceans (Guo et al., 2011). Consequently, more hot days and haze days have occurred, which threaten human health as well as social and economic activities (Ding et al., 2010; You et al., 2011; Chen et al., 2013; Ding and Liu, 2014; Wang et al., 2015). A further question is how the day-to-day variability (DDV) of the surface weather conditions over China have changed during the past several decades. The DDV of the surface weather conditions is a measure of the stability of the surface weather conditions (Rogers, 1997; Lehmann et al., 2014). With the trend towards a warmer and windless climate state, a stable surface weather condition may result in more persistent high-temperature and windless instances. These incidents feature consecutive warm and windless days and nights with no relief from muggy weather (Meehl and Tebaldi, 2004). This can have considerable impacts on human health. Despite numerous studies investigating climate change over China (e.g., Wu et al., 2010; Chen and Sun, 2015; He, 2015a; Sun and Wang, 2015; Feng and Chen, 2016; Shi et al., 2016), few studies have investigated the changes in

* Corresponding author: Bo SUN
Email: sunb@nuist.edu.cn

the DDV of the surface weather conditions over China, which is an important issue for the general population.

In the midlatitude regions, the DDV of the surface weather conditions is primarily influenced by the frequency and intensities of cyclonic and anticyclonic activity, i.e., synoptic-scale wave activity (Ulbrich et al., 2009). An increase (decrease) in the frequency and/or intensity of the cyclonic/anticyclonic activity would increase (decrease) the DDV of the weather conditions (Chang et al., 2002; Lehmann et al., 2014). The synoptic-scale wave activity is generally quantified by the variability of the sea level pressure (SLP) or geopotential height within a synoptic time range (e.g., 2–7 days), which provides a general view of the combined effects of the frequency and intensity of the cyclonic/anticyclonic activity (Yin, 2005; Ulbrich et al., 2009; Chen et al., 2014; Lehmann and Coumou, 2015). This quantity has frequently been used to denote storm tracks, where cyclones generate and/or propagate intensively (Ulbrich et al., 2009; Woollings et al., 2012; Nishii et al., 2015). Previous studies have suggested that the storm tracks in the Northern Hemisphere are undergoing a poleward shift in response to global warming and that the frequency of midlatitude cyclones is therefore decreasing (McCabe et al., 2001; Yin, 2005; Ulbrich et al., 2009). Fundamentally, the synoptic-scale wave activity in the midlatitudes depends on the baroclinic instability of the atmosphere, which is closely related to the meridional (equator-to-pole) temperature gradient (Shaw et al., 2016). It remains unclear what changes have occurred in the synoptic-scale wave activity and the baroclinic instability over China during the past several decades (Wang et al., 2009; Chen et al., 2014; Lehmann and Coumou, 2015).

To answer these questions, this study investigates the trends in the mean state and the DDV of the surface air temperatures and wind speeds over northern and northeastern China (NNEC) during 1961–2014 using observational data. Additionally, the trends are also examined in reanalysis data, and the underlying reasons for the changes in the DDV of the surface weather conditions explored.

The rest of this paper is organized as follows: Section 2 describes the data and methods used in the current study. In section 3, the trends in the mean state and the DDV of the surface air temperatures and wind speeds over NNEC are examined using observational and reanalysis data. Section 4 gives insight into the changes in the synoptic-scale wave activity and baroclinic instability, as well as their associated effects on the DDV of the surface heat flux. Section 5 investigates the underlying reason for the change in the baroclinic instability. A discussion is provided in section 6.

2. Data and methods

The observational data of the daily mean near-surface air temperature (Tm), daily maximum near-surface air temperature (Tmax), daily minimum near-surface air temperature (Tmin), and daily near-surface wind speed (sfcWind) in China used in this study are from the gridded CN05.1 dataset, which was constructed using data from 2400 observational stations in China, has a resolution of $0.25^\circ \times 0.25^\circ$, and a time span of 1961–2014 (Wu and Gao, 2013). The HadCRUT4 global temperature dataset is also used in this study, which has a resolution of $5^\circ \times 5^\circ$ and a time span of 1850–2016 (Morice et al., 2012).

The reanalysis data employed are from the National Centers for Environmental Prediction (NCEP) reanalysis dataset (Kalnay et al., 1996) and the 40-yr European Centre for Medium-Range Weather Forecasts Re-Analysis (ERA-40; Uppala et al., 2005). The time spans of the NCEP and ERA-40 data used in this study are 1961–2014 and 1961–2001, respectively.

Following Woollings et al. (2012) and Nishii et al. (2015), the current study uses the variance of 2–7-day bandpass filtered daily SLP (hereinafter SLP_var) to quantify the synoptic-scale wave activity. Accordingly, the variances of the 2–7-day bandpass filtered daily Tm, Tmin, Tmax, and sfcWind (hereinafter Tm_var, Tmin_var, Tmax_var, and sfcWind_var, respectively) were computed to quantify the DDV of the surface weather conditions. The 2–7-day bandpass filtering was performed using a Lanczos filter (Duchon, 1979).

In addition, the maximum Eady growth rate ($\sigma_{\rm BI}$) at 850–200 hPa was calculated to represent the baroclinic instability (Simmonds and Lim, 2009; Lehmann et al., 2014). The $\sigma_{\rm BI}$ is defined as

$$\sigma_{\rm BI} = 0.31 \frac{|f|}{N} \left| \frac{\partial U}{\partial z} \right| ,$$

where N is the Brunt–V*äisälä* frequency, f is the Coriolis parameter, U is the zonal wind, and z is the vertical height.

This study focuses on the midlatitude East Asian region (32°–58°N, 105°–135°E) that encompasses northern China (32°–41°N, 105°–120°E), northeastern China (41°–55°N, 115°–135°E), and the adjacent regions, as shown in Fig. 1.

3. Changes in the mean state and the DDV of the surface weather conditions

3.1. *Observational evidence*

Figure 1 shows the observed trends in the mean state and the DDV of the surface weather conditions over NNEC during 1961–2014. It can be seen that the Tm, Tmin, and Tmax over NNEC all experienced a significant increasing trend (Figs. 1a–c), whereas the sfcWind experienced a significant decreasing trend (Fig. 1d), demonstrating a tendency towards a warm and windless state over NNEC. The DDV of the Tm, Tmin, Tmax, and sfcWind consistently exhibits a decreasing trend in most areas of NNEC (Figs. 1e–h), indicating an increased stability of the surface weather conditions on the synoptic scale. This trend towards a stable warm and windless state implies increased risks of long-lasting hot and hazy days (Ding et al., 2010; Chen and Wang, 2015).

The time series for the areal mean values were computed to inspect the decadal variability. As shown in Figs. 2a–c, the temperature increased during 1971–99, was stable for a few

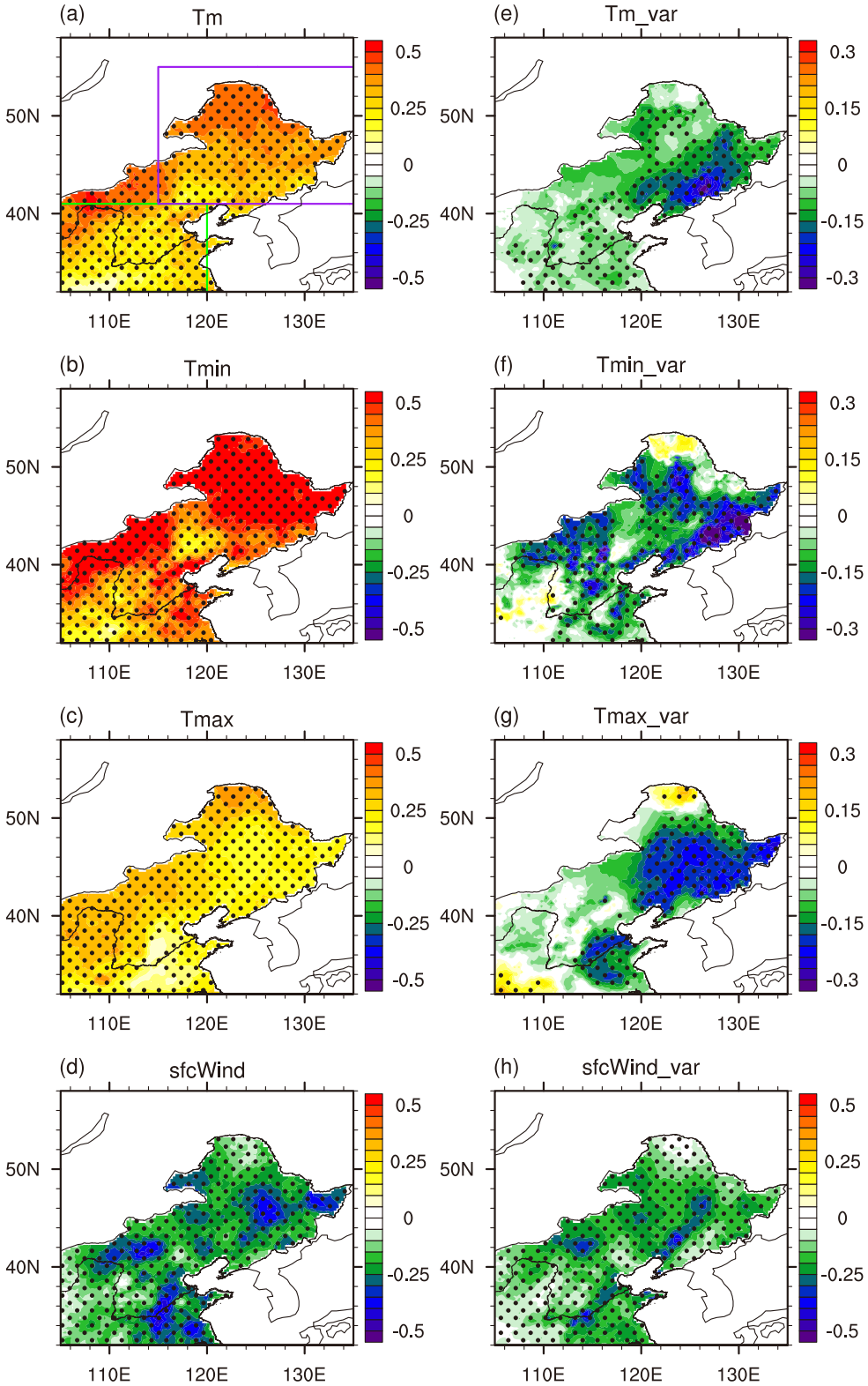

Fig. 1. Trends in the annual mean (a) Tm, (b) Tmin, (c) Tmax, and (d) sfcWind, and trends in the annual mean (e) Tm_var, (f) Tmin_var, (g) Tmax_var, and (h) sfcWind_var, during 1961–2014. The units of the trends in temperature (Tm, Tmin, Tmax) and temperature variance (Tm_var, Tmin_var, Tmax_var) are °C (10 yr)$^{-1}$ and °C^2 (10 yr)$^{-1}$, respectively; the units of the trends in sfcWind and sfcWind_var are m s^{-1} (10 yr)$^{-1}$ and m^2 s^{-2} (10 yr)$^{-1}$, respectively (the same for subsequent figures). Stippling denotes regions where the trends are at the 95% confidence level of the Student's *t*-test (the same for subsequent figures). The purple and green rectangles in (a) denote the ranges of northeastern China and northern China, respectively.

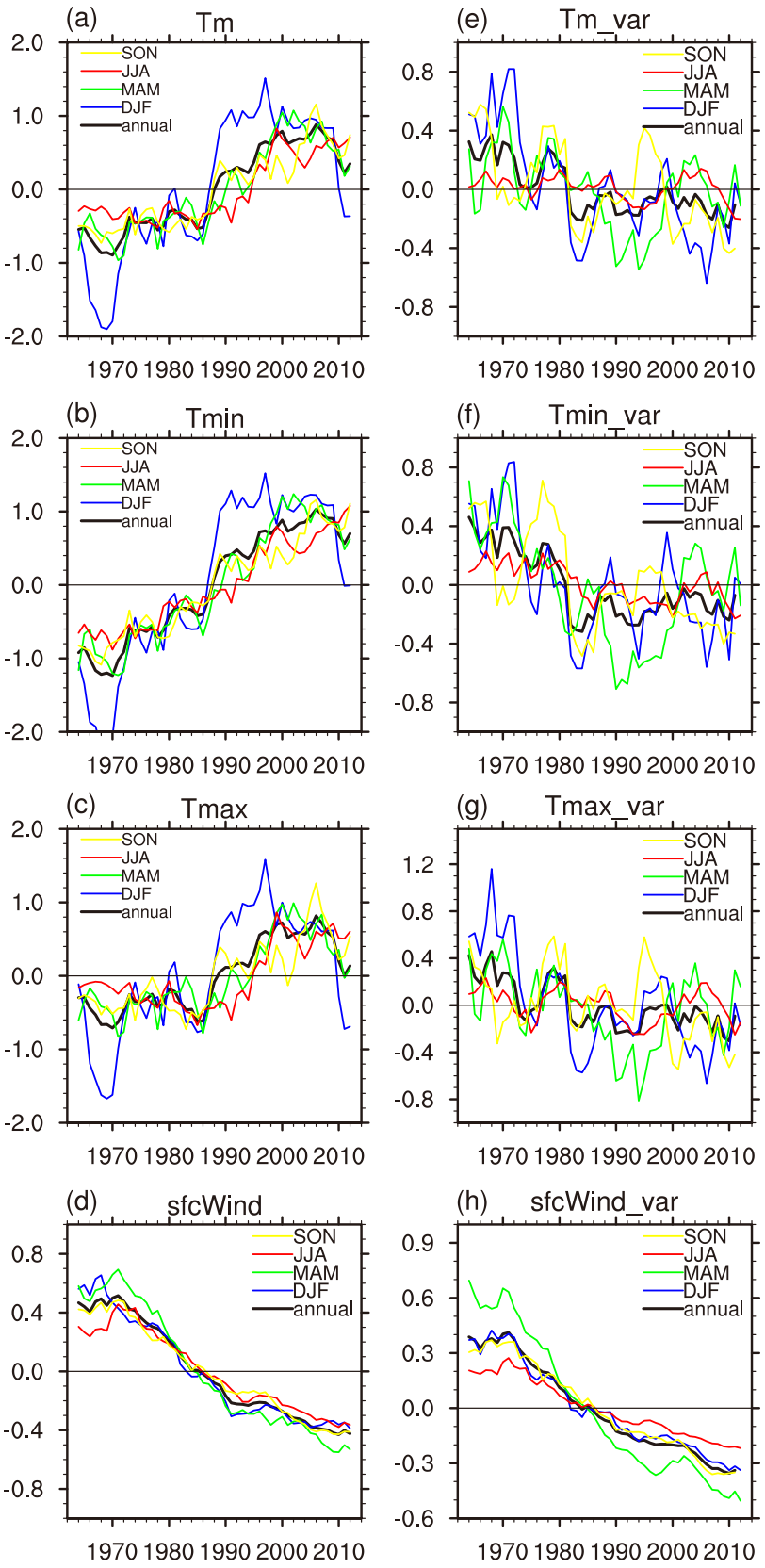

Fig. 2. Time series of the anomalies of the areal mean (a) Tm, (b) Tmin, (c) Tmax, and (d) sfcWind, and the areal mean (e) Tm_var, (f) Tmin_var, (g) Tmax_var, and (h) sfcWind_var, over NNEC. All the time series are smoothed by a 5-year running average. Units: °C for Tm, Tmin, and Tmax; m s^{-1} for sfcWind; $°C^2$ for Tm_var, Tmin_var, and Tmax_var; and m^2 s^{-2} for sfcWind_var.

years after entering the 21st century, and fell after 2009. A computation based on the HadCRUT4 dataset demonstrates a long-term increasing trend of the temperature over NNEC during 1850–2016, with a rapid increase in the 1980s and 1990s (figure not shown). The lack of warming over NNEC after 2000 may be related to the recent global warming hiatus in the early 21st century, which is likely due to the equatorial Pacific cooling during the past decade (Kosaka and Xie, 2013). The results from the HadCRUT4 dataset also indicate that the temperature over NNEC has recovered after a short cooling during 2009–13, the cause of which warrants further study. In contrast, the surface wind speed decreased rapidly during 1971–90, and continued to decrease at a slower rate after 1990 (Fig. 2d). For the DDV of the surface weather conditions, the annual mean DDV in the temperature noticeably decreased during 1961–90, and was stable after 1990 (Figs. 2e–g). In particular, the DDV in the temperature during the spring also notably decreased during 1961–90, but recovered to a moderate level afterwards. On the other hand, the DDV in the surface wind speed exhibits a remarkable and coherent decreasing trend from 1970 to the present (Fig. 2h).

The different features in the abovementioned decadal variations indicate the complexity of the surface weather conditions over NNEC. Considering that the DDV of both the surface temperatures and wind speeds is largely related to the synoptic-scale wave activity, it is somewhat unexpected to see that the DDV of the surface temperature remained stable after 1990, whereas the DDV of the surface wind speeds continued to decrease after 1990. This discrepancy may be due to multiple factors that influence the surface temperatures and winds. For instance, the DDV of the surface temperature is decided by the DDV of the surface heat budget, which is influenced by many factors, such as surface winds, solar radiation, cloud cover, and surface evaporation (Sun, 2017).

Both the trends in the mean state and the DDV of the surface temperatures and wind speeds show seasonalities that feature a relatively small trend in the summer (June–July–August, JJA) and a relatively large trend in the winter (December–January–February, DJF), spring (March–April–May, MAM), and autumn (September–October–November, SON), as shown in Fig. 3. Interestingly, the largest trend in Tmin_var and sfcWind_var occurs during the spring (Figs. 3f and h), whereas the largest trends in Tm_var and Tmax_var occur during the winter (Figs. 3e and g). The trends in the mean states of the surface temperatures and wind speeds are mostly consistent with the trends in the DDV of the surface temperatures and wind speeds with respect to their seasonality. However, it is not clear whether the seasonality of this trend in the mean state is linked to the seasonality of the trend in the DDV of the surface weather conditions. To answer this question, a deeper insight into what controls the seasonality of the trends in the mean state of temperature and winds and what controls the seasonality of the trends in the DDV of temperature and winds is needed.

3.2. *Trends in reanalysis data*

The changes in the mean state and the DDV of the surface weather conditions in the reanalysis data are examined for the NCEP and ERA-40 datasets. Both datasets show an increasing trend in the surface air temperature and a decreasing trend in the surface wind speeds over NNEC (Table 1). For both datasets, the magnitudes of the trends in the surface air temperature during the different seasons are comparable to those in the observational data, whereas the trends in the surface wind speeds are mostly insignificant and are smaller than the observed trends.

The DDV of the surface air temperature in the ERA-40 data assumes a significant decreasing trend during spring and a decreasing trend during other seasons, but with lower significance (Table 1). For the DDV of the surface wind speeds, the ERA-40 dataset does not show a significant trend during any season, although there are slight decreasing trends during the spring and autumn. The NCEP data show the decreasing trend in the DDV of the surface temperatures during the spring, and show an increasing trend over NNEC during the other seasons. Similar to the ERA-40 data, the DDV of the surface wind speeds in the NCEP data has no significant trend during any season, although it has slight decreasing trends during the spring, summer, and autumn.

Overall, the ERA-40 dataset shows the decreasing trend in the DDV of the surface temperature over NNEC more clearly than the NCEP dataset, and both datasets show a decreasing trend in the DDV of the surface weather conditions during the spring. Hence, in the following sections, our analysis is mainly focused on the spring to investigate the underlying reasons for the decreased DDV of the surface weather

Table 1. Linear trends in the mean state and the DDV of the surface weather conditions in the ERA-40 and NCEP data. The numbers not in brackets are for NNEC, excluding regions outside of China, and the numbers in brackets are for the entire (32°–58°N, 105°–135°E) region. The numbers in bold are significant at the 95% confidence level.

		DJF	MAM	JJA	SON	Annual
ERA-40 (1961–2001)	Tm [°C (10 yr)$^{-1}$]	**0.46 (0.40)**	**0.21 (0.27)**	0.06 (0.16)	0.19 (0.19)	**0.23 (0.25)**
	sfcWind [m s^{-1} (10 yr)$^{-1}$]	**−0.10 (−0.08)**	−0.03 (−0.01)	−0.01 (−0.02)	−0.03 (−0.01)	**−0.04 (−0.03)**
	Tm_var [°C^2 (10 yr)$^{-1}$]	−0.10 (−0.13)	**−0.22 (−0.17)**	−0.04 (−0.01)	−0.08 (−0.09)	**−0.11 (−0.10)**
	sfcWind_var [m^2 s^{-2} (10 yr)$^{-1}$]	0.03 (0.04)	−0.03 (−0.03)	−0.03 (−0.02)	0.03 (0.01)	0.00 (−0.00)
NCEP (1961–2014)	Tm [°C (10 yr)$^{-1}$]	**0.21** (0.23)	**0.18 (0.24)**	**0.22 (0.21)**	**0.17 (0.23)**	**0.20 (0.23)**
	sfcWind [m s^{-1} (10 yr)$^{-1}$]	−0.01 (−0.02)	−0.02 (−0.01)	**−0.09 (−0.07)**	−0.02 (−0.01)	**−0.03 (−0.03)**
	Tm_var [°C^2 (10 yr)$^{-1}$]	0.07 (−0.07)	−0.06 (**−0.16**)	**0.08** (0.04)	0.04 (−0.04)	0.03 (−0.06)
	sfcWind_var [m^2 s^{-2} (10 yr)$^{-1}$]	0.02 (0.01)	−0.01 (−0.02)	−0.02 (−0.02)	−0.01 (−0.01)	−0.00 (−0.01)

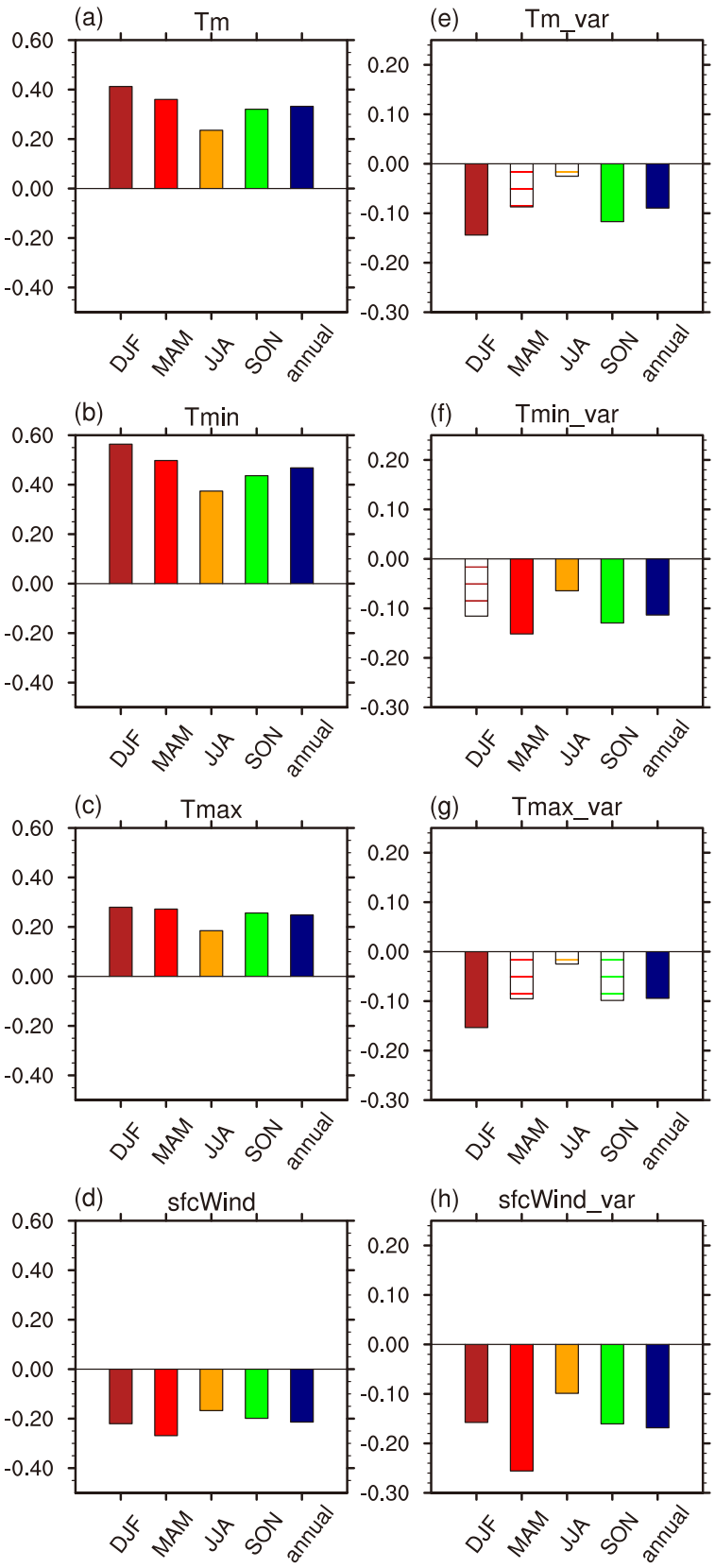

Fig. 3. Seasonality of the trends in the areal mean (a) Tm, (b) Tmin, (c) Tmax, and (d) sfcWind, and areal mean (e) Tm_var, (f) Tmin_var, (g) Tmax_var, and (h) sfcWind_var, over NNEC during 1961–2014. The bars filled with solid color indicate significance at the 95% confidence level, and the bars filled with lines indicate significance below the 95% confidence level (the same for subsequent figures).

conditions over NNEC. These reasons apply not only to the spring but also have important implications for the other seasons. Figure 4 compares the trends in the DDV of the surface temperatures during the spring in the observational and reanalysis data. A decreasing trend is detected over Mongolia and northeastern China in both the EAR-40 and NCEP datasets (Figs. 4b and c), which is consistent with the trend in the observational data (Fig. 4a). The decreasing trend over northern China in the observational data is shown in the ERA-40 data (Fig. 4b), but the NCEP data show an increasing trend here (Fig. 4c). This deviation in the NCEP data exists over northern China during all seasons. Thus, the NCEP data should be used with caution when investigating the trends or decadal variations in the DDV of the surface weather conditions over northern China. This error may be partially due to the lower quality of the NCEP data over the Asian region before the 1970s (Wu et al., 2005).

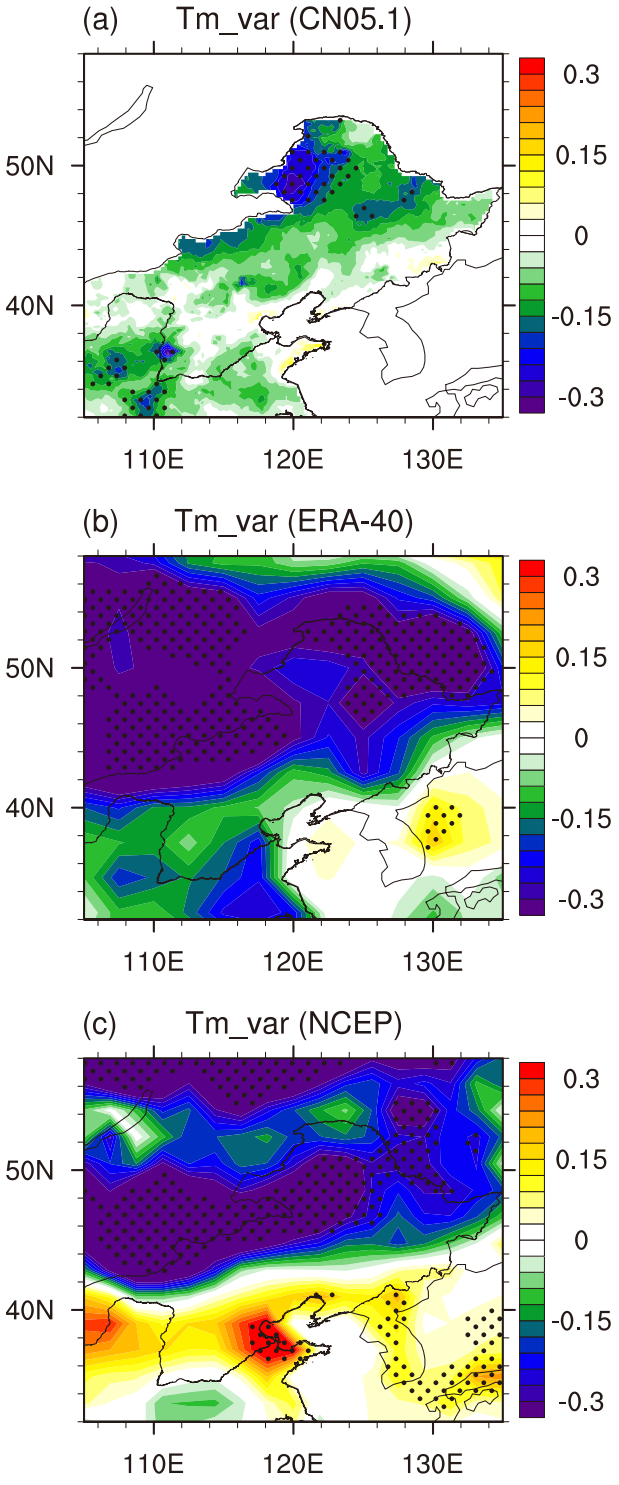

Fig. 4. Trends in Tm_var during the spring in the (a) observational data (1961–2014), (b) ERA-40 data (1961–2001), and (c) NCEP data (1961–2014).

4. Changes in the baroclinic instability and its associated effects on the DDV of the surface heat flux

4.1. *Changes in the synoptic-scale wave activity and baroclinic instability*

Changes in the DDV of the surface weather conditions are closely related to changes in synoptic-scale wave activity, which is a reflection of the atmospheric baroclinic instability. Therefore, the changes in the synoptic-scale wave activity and baroclinic instability during the spring were further examined to investigate the underlying reasons for the increased stability of the surface weather conditions over NNEC, as shown in Figs. 5 and 6. In both the ERA-40 and NCEP datasets, the synoptic-scale wave activity quantified by the DDV of SLP shows a decreasing trend over Mongolia and most parts of NNEC during the spring (Figs. 5a and c), indicating reduced cyclonic/anticyclonic activity. The trend over northern China is not as significant as that over Mongolia and northeastern China. Moreover, there is an increasing trend in the DDV of SLP over Bohai Bay and the adjacent oceanic regions. These features highlight a belt of decreased synoptic-scale wave activity between 40°N and 60°N over East Asia. The other seasons also show decreased synoptic-scale wave activity over this region. However, the trend during the spring is the largest of all the seasons (Figs. 5b and d), and occurs in concert with the largest decreasing trend in the DDV of the surface temperatures (Table 1).

It should be noted that the DDV of SLP is used as an indicator of the synoptic-scale wave activity. This does not necessarily mean that the DDV of SLP has a direct impact on the DDV of the surface weather conditions. In addition to the DDV of SLP, there are other indicators of the synoptic-scale wave activity, such as the eddy kinetic energy (EKE) and the DDV of geopotential height (Ulbrich et al., 2009; Lehmann et al., 2014). We also computed the trend in the EKE at 850 hPa and the trend in the DDV of the geopotential height at 500 hPa for the reanalysis data. The ERA-40 data exhibit a decreasing trend in the EKE and the DDV of the geopotential height over northeastern China during spring, which is consistent with the decreasing trend in the DDV of SLP. The NCEP data exhibit inconsistent trends in these three indicators of synoptic-scale wave activity, with insignificant trends in the EKE and the DDV of the geopotential height during

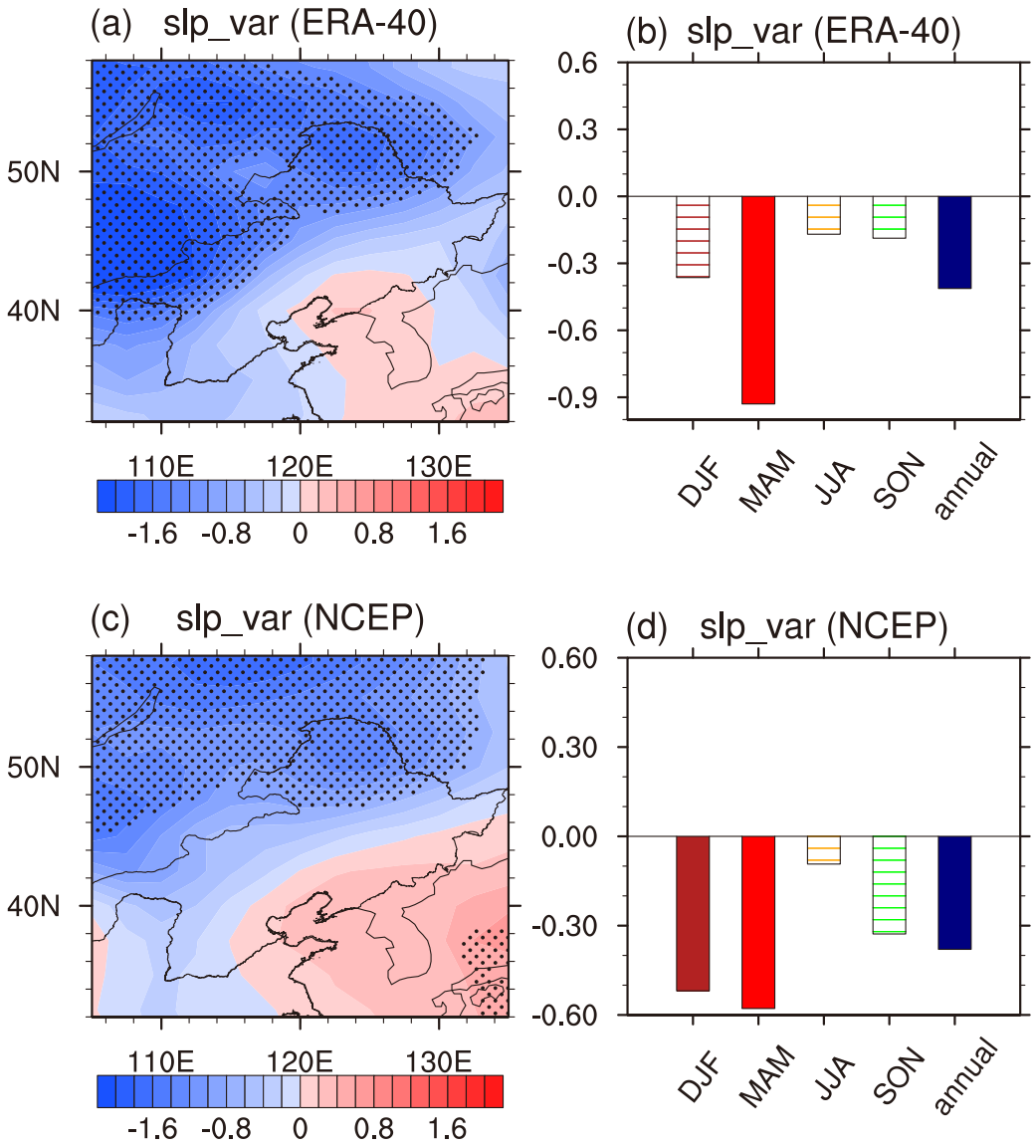

Fig. 5. Trends in SLP_var during the spring in the (a) ERA-40 and (c) NCEP data. Seasonality of the areal mean trends in SLP_var over the region (32°–58°N, 105°–135°E) during the spring in the (b) ERA-40 and (d) NCEP data. Units: hPa^2 $(10\ yr)^{-1}$.

the spring. With this in mind, it seems that the ERA-40 data are more useful than the NCEP data for analysis of the trend and decadal variations in the DDV of weather conditions over East Asia.

The aforementioned decreased synoptic-scale wave activity implies a decreased atmospheric baroclinic instability over the midlatitudes of East Asia, which is further shown by the change in the maximum Eady growth rate (Fig. 6). As shown in Fig. 6, both the ERA-40 and NCEP datasets demonstrate a decreasing trend in the baroclinic instability over the East Asian regions between 40°N and 60°N during the spring. On the other hand, an increasing trend in the baroclinic instability is identified over the regions south of 40°N. This contrasting change in baroclinic instability is most significant in the upper-level (500–200 hPa) atmosphere. In the lower- and middle-level (850–500 hPa) atmosphere, the trend in the baroclinic instability is mainly characterized by a decreasing trend over Mongolia and northeastern China. The changes in the baroclinic instability are closely related to the meridional temperature gradient, which is discussed in section 5.

4.2. *Changes in the DDV of the surface heat flux*

A decreased synoptic-scale wave activity, which signifies a decreased frequency and/or intensity of cyclonic/anticyclonic activities, would cause a decreased DDV of atmospheric variables, such as cloud cover and winds, and vice versa (Chang et al., 2002; Lehmann et al., 2014). Thus, the baroclinic instability and synoptic-scale wave activity can affect the DDV of the surface wind speeds directly by

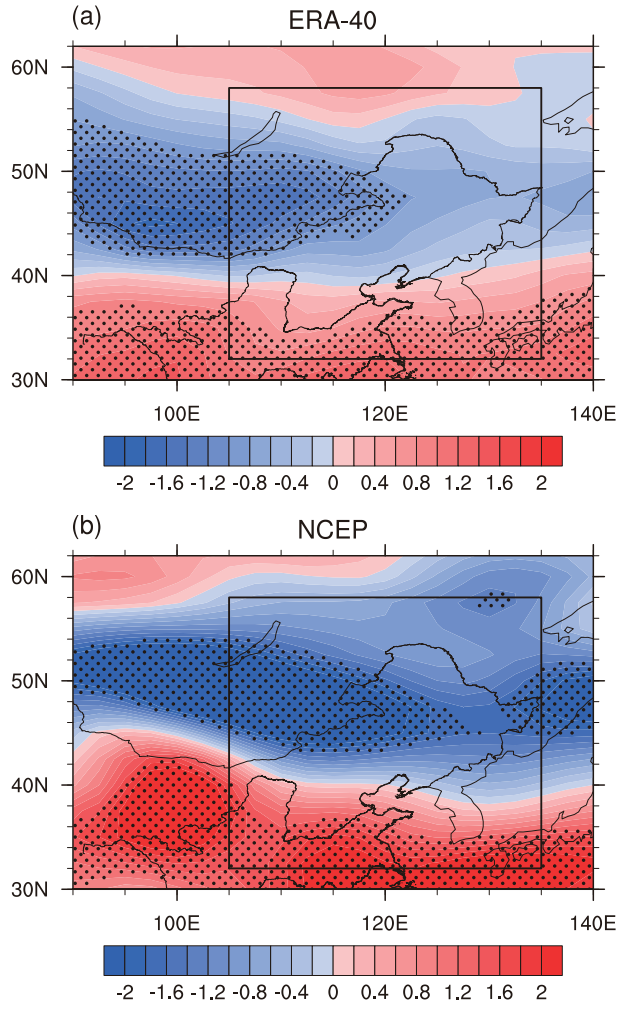

Fig. 6. Trends in the maximum Eady growth rate (850–200 hPa) in the (a) ERA-40 and (b) NCEP data. Units: s^{-1} $(10\ yr)^{-1}$. The black rectangle denotes the target domain of this study.

modulating the DDV of the low-level winds (Table 1), and can affect the DDV of the surface temperatures by modulating the DDV of the surface heat flux, which is influenced by several factors, including cloud cover and wind-driven thermal advection (Chen et al., 2016; Sun, 2017).

Figure 7 shows the trends in the DDV of surface heat fluxes during the spring in the ERA-40 data, indicating an overall decreasing trend in NNEC. Specifically, the DDV of the surface net short-wave radiation (SWR) and the DDV of the surface sensible heat flux (SHF) show relatively strong decreasing trends over NNEC (Figs. 7a and b). Cloud and snow cover are two of the main factors influencing the surface SWR (Sun, 2017). Considering that cloud cover is much more variable than snow cover on the synoptic scale, the decreased DDV of the surface SWR may largely be attributed to a decreased DDV of the cloud-forced SWR. The decreasing trend in the DDV of the surface SHF is likely due to a decreased DDV of the surface wind-driven thermal advection (Ye et al., 2015). The DDV of the surface net long-wave radiation (LWR) also exhibits a decreasing trend over NNEC (Fig. 7c), which may be mainly caused by a decreased DDV of the cloud-forced LWR. For the DDV of the surface latent heat flux (LHF), a slight decreasing trend is detected over NNEC (Fig. 7d), which is likely due to a decreased DDV of the surface wind speeds (Table 1; Sun, 2017). Consequently, a decreasing trend in the DDV of the surface net heat flux (NHF) is observed over NNEC (Fig. 7e). The trends of the DDV of the SWR, LWR, SHF, and LHF over the NNEC region (excluding regions outside of China) are −41.2, −5.3, −13.5, and −2.4 $W^2\ m^{-4}\ (10\ yr)^{-1}$, respectively. These results imply that the decreasing DDV of the SWR makes an important contribution to the decreasing trend in the DDV of the temperature, and that the decreasing DDV of the SHF makes a secondary contribution. Furthermore, we computed the time series of the DDV of the temperature and surface heat fluxes, and their corresponding correlation coefficients. These results indicate that the interannual and decadal variability of the DDV of the temperature is closely linked to the DDV of the SHF. Specifically, the result based on a 15-year running mean time series implies that the DDVs of both the SWR and SHF are important contributors to the decreasing trend of the DDV of the temperature.

The DDV of the surface NHF in the NCEP data shows a decreasing trend over Mongolia and northeastern China, which is related to a decreased DDV of the surface SWR (figure not shown). Using the NCEP cloud forcing SWR and cloud forcing LWR data, it is clear that the decreased DDVs of the surface SWR and LWR are mainly due to the decreased DDVs of the cloud-forced SWR and LWR, respectively.

5. Changes in temperature gradient

Fundamentally, the energy behind the atmospheric baroclinic instability and cyclonic/anticyclonic activities in the midlatitude regions is the potential energy associated with the meridional temperature gradient (Eady, 1949; Charney and Stern, 1962). The meridional temperature gradient also leads to horizontal and vertical wind shear over the midlatitudes (Charney and Stern, 1962).

To investigate the reason for the decreased baroclinic instability over the midlatitudes of East Asia, an insight into the meridional temperature gradient is needed. Figure 8 shows the trend in air temperature over East Asia (90°–140°E) at different pressure levels, with similar results obtained from the EAR-40 and NCEP data. The air temperature over the midlatitude regions surrounding approximately 40°N decreases for 700–250 hPa, whereas the air temperature over the higher latitude regions increases for 1000–300 hPa (Figs. 8a and c). As such, the meridional temperature gradient is reduced over the higher latitude regions at 40°–60°N and is enlarged over the lower latitude regions at 20°–40°N. Consequently, the atmospheric baroclinic instability decreases (increases) over the East Asian regions north (south) of 40°N (Fig. 6). In addition, the vertical wind shear is weakened at 40°–60°N and is strengthened at 20°–40°N (Figs. 8b and d). The increased vertical wind shear at 20°–40°N results in an

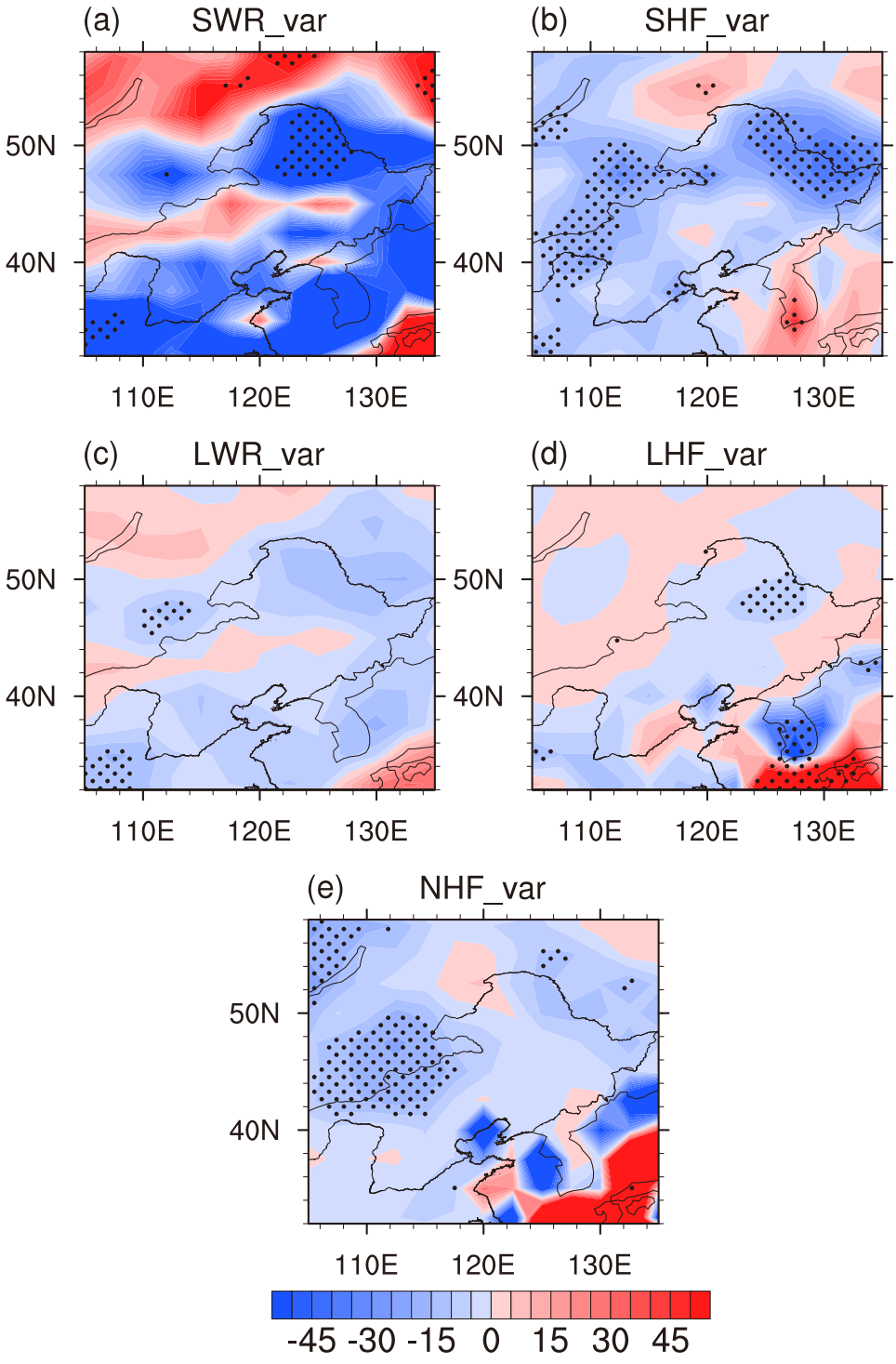

Fig. 7. Trends in the DDV of the surface (a) SWR, (b) SHF, (c) LWR, (d) LHF, and (e) NHF during the spring for the ERA-40 data. The NHF is calculated using NHF = SWR + SHF + LWR + LHF. Units: $W^2\ m^{-4}\ (10\ yr)^{-1}$.

enhanced East Asian upper-tropospheric jet stream, which is closely related to the weather and climate in East Asia (Yang et al., 2002; Lin and Lu, 2005). The results are essentially the same as for the 105°–135°E longitude range.

The cooling trend in the middle-to-upper tropospheric atmosphere at approximately 40°N plays a key role in the contrasting changes of the baroclinic instability to the north and south of 40°N. As shown in Fig. 9, the cooling in the upper-tropospheric atmosphere during the spring is centered around (40°N, 100°E) and extends from West China to East China, forming a sharp contrast with the surrounding insignificant and/or increasing trends in air temperature. This cooling zone

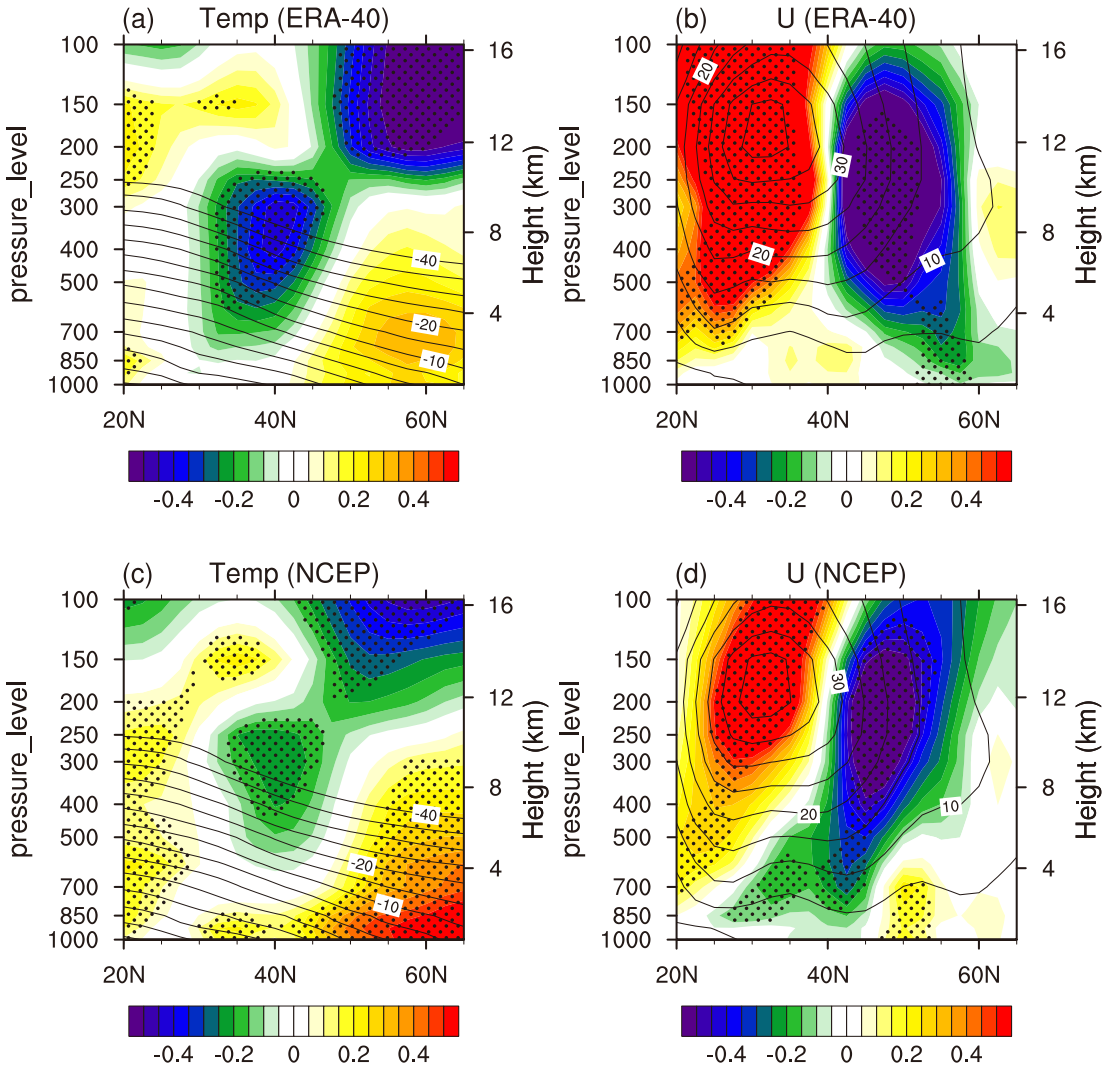

Fig. 8. Latitude–pressure section of the trends (color shading) in 90°–140°E averaged (a, c) air temperature [units: °C (10 yr)$^{-1}$] and (b, d) zonal wind [units: m s^{-1} (10 yr)$^{-1}$] during the spring in the (a, b) ERA-40 and (c, d) NCEP data. The contour lines denote the corresponding climatology of the temperature (units: °C) and the zonal winds during the spring (units: m s^{-1}). Units of pressure level (left vertical axis): hPa.

is also detected during other seasons in the reanalysis data, with relatively small trends in temperature. The location and strength of this cooling zone could substantially influence the meridional temperature gradient and thus the baroclinic instability over East Asia. Hypothetically, this cooling zone may also partially account for the observed decreasing trend in the DDV of the surface weather conditions over NNEC for other seasons, although this is not well represented in the reanalysis data. In addition, it has also been suggested that the tropospheric cooling over East Asia is responsible for the weakening of the East Asian summer monsoon and the spring drought in southeastern China in recent decades (Yu et al., 2004; Xin et al., 2008).

But what causes the tropospheric cooling over East Asia? A possible mechanism for this is the increased snow depth over the Tibetan Plateau during winter, cooling the Tibetan Plateau during winter and spring, which induces gravity waves to propagate upwards and northwards into the stratosphere and causes tropospheric cooling north of the Tibetan Plateau through stratosphere–troposphere interaction (Yu et al., 2004; Xin et al., 2010). However, the observational evidence indicates that the Tibetan Plateau has undergone a significant warming trend from 1961 to the present (Wang et al., 2008; Guo and Wang, 2011). Thus, the above mechanism needs further examination. Another possible mechanism is that the ozone depletion over the Tibetan Plateau causes stratospheric cooling and results in tropospheric cooling over East Asia through stratosphere–troposphere interaction (Yu et al., 2004; Zhou and Zhang, 2005). During the past several decades, the global lower stratosphere has been cooled by both natural factors and anthropogenic factors, such as ozone depletion and the increase in greenhouse gases (Ramaswamy et al., 2006). The upper-tropospheric cooling over East Asia is likely a consequence of ozone depletion and

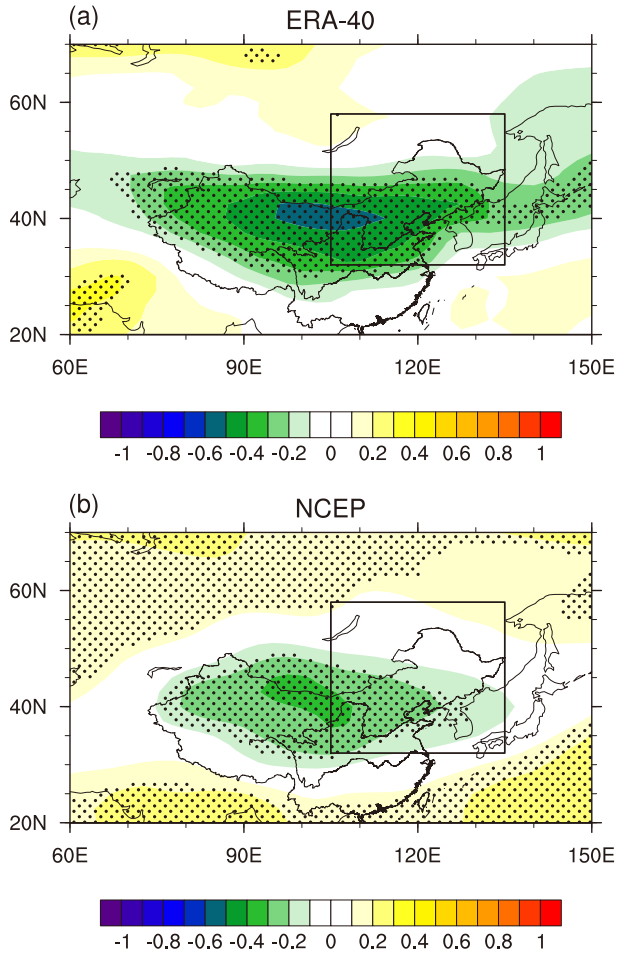

Fig. 9. Trend in the 300 hPa air temperatures for the (a) ERA-40 and (b) NCEP data. Units: °C (10 yr)$^{-1}$.

the increased greenhouse gas emissions over Asia. However, further studies are needed to better understand this issue.

6. Discussion

This study mainly focuses on the relationship between the DDV of the surface weather conditions and the synoptic-scale wave activity over NNEC. A decreasing trend in the DDV of the surface wind speeds with smaller magnitudes is also observed in regions of mainland China other than NNEC. This general decrease in the DDV of the surface wind speeds over China is coincident with a general decrease in the surface wind speeds over China that is not only related to the change in the pressure/temperature gradient but is also related to urbanization in China (Guo et al., 2011).

During the winter, the East Asian trough has a remarkable impact on the weather in East Asia (Gong et al., 2001). It has been suggested that a positive- (negative-) phase Arctic Oscillation (AO) is concurrent with a weakened (strengthened) East Asian trough (He et al., 2017). The AO index experienced a trend towards a positive phase during 1961–2014, which may have impacted the weather and climate of East Asia by modulating the East Asian trough (He, 2015b). The relationship between the AO and the DDV of the surface weather conditions in East Asia should be studied further.

The ability of the reanalysis data to represent the synoptic-scale variability of the weather conditions also needs further examination. This study suggests a better qualification of the ERA-40 data for analyzing the DDV of the weather conditions over East Asia. Further analysis of the frequency and intensity of cyclones and anticyclones is needed for a comprehensive understanding of the changes in the synoptic activity in the reanalysis data (Chen et al., 2014). This study did not explore why the ERA-40 and NCEP reanalysis data show a consistent decreasing trend in the DDV of the surface weather conditions only in the spring. The reanalysis data may have different abilities during different seasons due to a variety of potential factors of influence associated with the observational database and the assimilating model (Kalnay et al., 1996; Bromwich and Fogt, 2004; Simmons et al., 2004; Uppala et al., 2005; Bromwich et al., 2007). Further studies are needed to answer this question.

Finally, we compared the results from the JRA-55 dataset (Kobayashi et al., 2015) with the results of the ERA-40 and NCEP data. At first, it was surprising to see that the JRA-55 data show a decreasing trend in the DDV of the surface temperatures and wind speeds for all seasons, suggesting a notably better accuracy than the ERA-40 and NCEP data. However, this might be because the surface temperature and wind in the JRA-55 data are analyzed based on a correction of the first guess made by comparing the first guess with observational data (Kobayashi et al., 2015). The results from the other fields of the JRA-55 data are similar to the ERA-40 and NCEP data for the spring and do not show a significant difference from the ERA-40 and NCEP data for the other seasons. The better performance of the JRA-55 data in representing the decreasing trend of the DDV of surface weather conditions cannot be reasonably explained from a perspective of atmospheric dynamics. For instance, the DDV of surface temperature in the JRA-55 data shows a significant decreasing trend over NNEC during the winter, which mimics the observed trend, whereas the DDV of surface net heat flux in the JRA-55 data shows an insignificant trend over NNEC during the winter. Thus, the better skill of the JRA-55 might be attributable to the correction of the first guess of the modeled surface temperatures and winds. However, this is just a preliminary hypothesis. A better understanding of this question will require further study.

Acknowledgements. This study was supported by the National Natural Science Foundation of China (Grant Nos. 41421004 and 41210007) and the Atmosphere-Ocean Research Center (AORC) and International Pacific Research Center (IPRC) at University of Hawaii. We thank the three anonymous reviewers for their comments.

REFERENCES

Bromwich, D. H., and R. L. Fogt, 2004: Strong trends in the skill of the ERA-40 and NCEP NCAR Reanalyses in the high and

midlatitudes of the Southern Hemisphere, 1958–2001. *J. Climate*, **17**, 4603–4619.

Bromwich, D. H., R. L. Fogt, K. I. Hodges, and J. E. Walsh, 2007: A tropospheric assessment of the ERA-40, NCEP, and JRA-25 global reanalyses in the polar regions. *J. Geophys. Res.*, **112**, D10111, doi: 10.1029/2006JD007859.

Chang, E. K. M., S. Lee, and K. L. Swanson, 2002: Storm track dynamics. *J. Climate*, **15**, 2163–2183.

Charney, J. G., and M. E. Stern, 1962: On the stability of internal baroclinic jets in a rotating atmosphere. *J. Atmos. Sci.*, **19**, 159–172.

Chen, H. P., and H. J. Wang, 2015: Haze days in North China and the associated atmospheric circulations based on daily visibility data from 1960 to 2012. *J. Geophys. Res.*, **120**, 5895–5909, doi: 10.1002/2015JD023225.

Chen, H. P., and J. Q. Sun, 2015: Changes in climate extreme events in China associated with warming. *Int. J. Climatol.*, **35**, 2735–2751.

Chen, L., B. K. Tan, N. G. Kvamstø, and O. M. Johannessen, 2014: Wintertime cyclone/anticyclone activity over China and its relation to upper tropospheric jets. *Tellus A*, **66**, 21889, http://dx.doi.org/2188910.3402/tellusa.v66.21889.

Chen, S. F., W. Chen, and K. Wei, 2013: Recent trends in winter temperature extremes in Eastern China and their relationship with the Arctic Oscillation and ENSO. *Adv. Atmos. Sci.*, **30**, 1712–1724, doi: 10.1007/s00376-013-2296-8.

Chen, S. F., R. G. Wu, and Y. Liu, 2016: Dominant modes of interannual variability in Eurasian surface air temperature during boreal spring. *J. Climate*, **29**, 1109–1125, doi: 10.1175/JCLI-D-15-0524.1.

Ding, T., W. H. Qian, and Z. W. Yan, 2010: Changes in hot days and heat waves in China during 1961-2007. *Int. J. Climatol.*, **30**, 1452–1462, doi: 10.1002/joc.1989.

Ding, Y. H., and Y. J. Liu, 2014: Analysis of long-term variations of fog and haze in China in recent 50 years and their relations with atmospheric humidity. *Science China Earth Sciences*, **57**, 36–46, doi: 10.1007/s11430-013-4792-1.

Ding, Y. H., G. Y. Ren, Z. C. Zhao, Y. Xu, Y. Luo, Q. P. Li, and J. Zhang, 2007: Detection, causes and projection of climate change over China: An overview of recent progress. *Adv. Atmos. Sci.*, **24**, 954–971, doi: 10.1007/s00376-007-0954-4.

Duchon, C. E., 1979: Lanczos filtering in one and two dimensions. *Journal of Applied Meteorology*, **18**, 1016–1022.

Eady, E. T., 1949: Long waves and cyclone waves. *Tellus*, **1**, 33–52, http://dx.doi.org/10.1111/j.2153-3490.1949.tb01265.x.

Feng, Y., and H.-P. Chen, 2016: Warming over the North Pacific can intensify snow events in Northeast China. *Atmos. Oceanic Sci. Lett.*, **9**, 122–128.

Gong, D.-Y., S.-W. Wang, and J.-H. Zhu, 2001: East Asian winter monsoon and Arctic Oscillation. *Geophys. Res. Lett.*, **28**, 2073–2076.

Guo, D. L., and H. J. Wang, 2011: The significant climate warming in the northern Tibetan Plateau and its possible causes. *Int. J. Climatol.*, **32**, 1775–1781.

Guo, H., M. Xu, and Q. Hu, 2011: Changes in near-surface wind speed in China: 1969-2005. *Int. J. Climatol.*, **31**, 349–358.

He, S.-P, 2015a: Potential connection between the Australian summer monsoon circulation and summer precipitation over central China. *Atmos. Oceanic Sci. Lett.*, **8**, 120–126, doi: 10.3878/AOSL20140091.

He, S.-P., 2015b: Asymmetry in the arctic oscillation teleconnection with January cold extremes in Northeast China. *Atmos. Oceanic Sci. Lett.*, **8**, 386–391.

He, S. P., Y. Q. Gao, F. Li, H. J. Wang, and Y. C. He, 2017: Impact of Arctic Oscillation on the East Asian climate: A review. *Earth-Science Reviews*, **164**, 48–62.

Ji, F., Z. H. Wu, J. P. Huang, and E. P. Chassignet, 2014: Evolution of land surface air temperature trend. *Nature Climate Change*, **4**, 462–466, doi: 10.1038/NCLIMATE2223

Kalnay, E., and Coauthors, 1996: The NCEP/NCAR 40-year reanalysis project. *Bull. Amer. Meteor. Soc.*, **77**, 437–471.

Kobayashi, S., and Coauthors, 2015: The JRA-55 reanalysis: General specifications and basic Characteristics. *J. Meteor. Soc. Japan.*, **93**, 5–48.

Kosaka, Y., and S.-P. Xie, 2013: Recent global-warming hiatus tied to equatorial Pacific surface cooling. *Nature*, **501**, 403–407, doi: 10.1038/nature12534.

Lehmann, J., D. Coumou, K. Frieler, A. V. Eliseev, and A. Levermann, 2014: Future changes in extratropical storm tracks and baroclinicity under climate change. *Environ. Res. Lett.*, **9**, 084002, doi: 10.1088/1748-9326/9/8/084002.

Lehmann, J., and D. Coumou, 2015: The influence of mid-latitude storm tracks on hot, cold, dry and wet extremes. *Sci. Rep.*, **5**, 17491, doi: 10.1038/srep17491.

Lin, C. G., K. Yang, J. Qin, and R. Fu, 2013: Observed coherent trends of surface and upper-air wind speed over China since 1960. *J. Climate*, **26**, 2891–2903, doi: 10.1175/JCLI-D-12-00093.1

Lin, Z. D., and R. Y. Lu, 2005: Interannual meridional displacement of the East Asian upper-tropospheric jet stream in summer. *Adv. Atmos. Sci.*, **22**, 199–211, doi: 10.1007/BF02918509.

McCabe, G. J., M. P. Clark, and M. C. Serreze, 2001: Trends in Northern Hemisphere surface cyclone frequency and intensity. *J. Climate*, **14**, 2763–2768.

Meehl, G. A., and C. Tebaldi, 2004: More intense, more frequent, and longer lasting heat waves in the 21st century. *Science*, **305**, 994–997, doi: 10.1126/science.1098704.

Morice, C. P., J. J. Kennedy, N. A. Rayner, and P. D. Jones, 2012: Quantifying uncertainties in global and regional temperature change using an ensemble of observational estimates: The HadCRUT4 data set. *J. Geophys. Res.*, **117**, D08101, doi: 10.1029/2011JD017187.

Nishii, K., H. Nakamura, and Y. J. Orsolini, 2015: Arctic summer storm track in CMIP3/5 climate models. *Climate Dyn.*, **44**, 1311–1327, doi: 10.1007/s00382-014-2229-y.

Ramaswamy, V., M. D. Schwarzkopf, W. J. Randel, B. D. Santer, B. J. Soden, and G. L. Stenchikov, 2006: Anthropogenic and natural influences in the evolution of lower stratospheric cooling. *Science*, **311**, 1138–1141.

Rogers, J. C., 1997: North Atlantic storm track variability and its association to the North Atlantic Oscillation and climate variability of Northern Europe. *J. Climate*, **10**, 1635–1647.

Shaw, T. A., and Coauthors, 2016: Storm track processes and the opposing influences of climate change. *Nature Geoscience*, **9**, 656–665, doi: 10.1038/NGEO2783.

Shi, Y., X. J. Gao, Y. Xu, F. Giorgi, and D. L. Chen, 2016: Effects of climate change on heating and cooling degree days and potential energy demand in the household sector of China. *Climate Research*, **67**, 135–149, doi: 10.3354/cr01360.

Simmonds, I., and E.-P. Lim, 2009: Biases in the calculation of Southern Hemisphere mean baroclinic eddy growth rate. *Geophys. Res. Lett.*, **36**, L01707, doi: 10.1029/2008GL036320.

Simmons, A. J., and Coauthors, 2004: Comparison of

trends and low-frequency variability in CRU, ERA-40, and NCEP/NCAR analyses of surface air temperature. *J. Geophys. Res*., **109**, D24115, doi: 10.1029/2004JD005306.

Sun, B., 2017: Seasonal evolution of the dominant modes of the Eurasian snowpack and atmospheric circulation from autumn to the subsequent spring and the associated surface heat budget. *Atmos. Oceanic Sci. Lett.*, 10.1080/16742834.2017.1286226.

Sun, B., and H. J. Wang, 2015: Inter-decadal transition of the leading mode of inter-annual variability of summer rainfall in East China and its associated atmospheric water vapor transport. *Climate Dyn*., **44**, 2703–2722, doi: 10.1007/s00382-014-2251-0.

Ulbrich, U., G. C. Leckebusch, and J. G. Pinto, 2009: Extra-tropical cyclones in the present and future climate: A review. *Theor. Appl. Climatol*., **96**, 117–131, doi: 10.1007/s00704-008-0083-8.

Uppala, S. M., and Coauthors, 2005: The ERA-40 re-analysis. *Quart. J. Roy. Meteor. Soc*., **131**, 2961–3012.

Wang, B., Q. Bao, B. Hoskins, G. X. Wu, and Y. M. Liu, 2008: Tibetan Plateau warming and precipitation changes in East Asia. *Geophys. Res. Lett*., **35**, L14702, doi: 10.1029/2008GL034330.

Wang, H.-J., H.-P. Chen, and J. Liu, 2015: Arctic sea ice decline intensified haze pollution in Eastern China. *Atmos. Oceanic Sci. Lett.*, **8**, 1–9, doi: 10.3878/AOSL20140081.

Wang, X. M., P. M. Zhai, and C. C. Wang, 2009: Variations in extratropical cyclone activity in Northern East Asia. *Adv. Atmos. Sci*., **26**, 471–479, doi: 10.1007/s00376-009-0471-8.

Woollings, T., J. M. Gregory, J. G. Pinto, M. Reyers, and D. J. Brayshaw, 2012: Response of the North Atlantic storm track to climate change shaped by ocean-atmosphere coupling. *Nature Geoscience*, **5**, 313–317, doi: 10.1038/NGEO1438.

Wu, J., and X. J. Gao, 2013: A gridded daily observation dataset over China region and comparison with the other datasets. *Chinese Journal of Geophysics*, **56**, 1102–1111, doi: 10.6038/cjg20130406. (in Chinese)

Wu, J., X. Gao, F. Giorgi, and D. Chen, 2017: Changes of effective temperature and cold/hot days in late decades over China based on a high resolution gridded observation dataset. *Int. J. Climatol.*, doi: 10.1002/joc.5038.

Wu, R. G., J. L. Kinter III, and B. P. Kirtman, 2005: Discrepancy of interdecadal changes in the Asian region among the NCEP-NCAR reanalysis, objective analyses, and observations. *J. Climate*, **18**, 3048–3067.

Wu, R. G., Z. P. Wen, S. Yang, Y. Q. Li, 2010: An interdecadal change in Southern China summer rainfall around 1992/93. *J. Climate*, **23**, 2389–2403.

Xin, X. G., Z. X. Li, R. C. Yu, and T. J. Zhou, 2008: Impacts of upper tropospheric cooling upon the late spring drought in East Asia simulated by a regional climate model. *Adv. Atmos. Sci*., **25**, 555–562, doi: 10.1007/s00376-008-0555-x.

Xin, X. G., T. J. Zhou, and R. C. Yu, 2010: Increased Tibetan Plateau snow depth: An indicator of the connection between enhanced winter NAO and late-spring tropospheric cooling over East Asia. *Adv. Atmos. Sci*., **27**, 788–794, doi: 10.1007/s00376-009-9071-x.

Yang, S., K.-M. Lau, and K.-M. Kim, 2002: Variations of the East Asian jet stream and Asian-Pacific-American winter climate anomalies. *J. Climate*, **15**, 306–325.

Ye, K. H., R. G. Wu, and Y. Liu, 2015: Interdecadal change of Eurasian snow, surface temperature, and atmospheric circulation in the late 1980s. *J. Geophys. Res*., **120**, 2738–2753, doi: 10.1002/2015JD023148.

Yin, J. H., 2005: A consistent poleward shift of the storm tracks in simulations of 21st century climate. *Geophys. Res. Lett*., **32**, L18701, doi: 10.1029/2005GL023684.

You, Q. L., and Coauthors, 2011: Changes in daily climate extremes in China and their connection to the large scale atmospheric circulation during 1961–2003. *Climate Dyn*., **36**, 2399–2417.

Yu, R. C., B. Wang, and T. J. Zhou, 2004: Tropospheric cooling and summer monsoon weakening trend over East Asia. *Geophys. Res. Lett*., **31**, L22212, doi: 10.1029/2004GL021270.

Zhao, P., P. Jones, L. J. Cao, Z. W. Yan, S. Y. Zha, Y. N. Zhu, Y. Yu, and G. L. Tang, 2014: Trend of surface air temperature in Eastern China and associated large-scale climate variability over the last 100 years. *J. Climate*, **27**, 4693–4703, doi: 10.1175/JCLI-D-13-00397.1.

Zhou, S. W., and R. H. Zhang, 2005: Decadal variations of temperature and geopotential height over the Tibetan Plateau and their relations with Tibet ozone depletion. *Geophy. Res. Lett*., **32**, L18705, doi: 10.1029/2005GL023496.